UNIJOURN

*International Journal of Sustainable Transportation Technology*
*Vol. 3, No. 2, October 2020, 51-57*


# Al Ions Doping Effect on The Diffusion Coefficient and Capacity of $Li_4Ti_5O_{12}$ (Lithium Titanate, LTO) in Lithium-Ion Battery Anode

**Slamet Priyono[1*], Lufthansyah Daniswara[2], Rahma Alfia Khoiri[2], Yayuk Astuti[2,3*]**

[1]Research Center for Physics - Indonesian Institute of Sciences, Puspiptek, South Tangerang, Banten, Indonesia
[2]Chemistry Department, Faculty of Sciences and Mathematics, Diponegoro University, Semarang, Indonesia
[3]National Center for Sustainable Transportation Technology (NCSTT), Bandung, Indonesia
**Email: slam013@lipi.go.id*

**Abstract**

$Li_4Ti_5O_{12}$ (LTO) anode doped with Al ions with varying concentrations (Al = 0; 0.005; 0.015; 0.03; 0.045) was successfully synthesized using the sol-gel method. Al-doped LTO samples were obtained through the sintering of gel at 850°C for 4 hours under a normal atmosphere. Electrochemical performance such as charge-discharge capacity and diffusion coefficient were characterized using an automatic battery cycler. The cells consist of electrode sheets (LTO doping Al) as a working electrode, lithium metal as the counter electrode, Celgard film as the separator, and $LiPF_6$ as an electrolyte. Cyclic voltammetry test results show that a greater scan rate results in decreased capacity and greater polarization voltage. In addition, an increase in concentrations used in Al doping on LTO causes capacity, and the diffusion coefficient tends to decrease.

**Keywords**

*$Li_4Ti_5O_{12}$; Sol-gel; Aluminum doping; Lithium-ion battery; Electrochemical performance*

## 1 Introduction

The utilization of electronic parts in the ever-developing new technologies such as laptops, personal gadgets, and electric cars is increasing [1]. The trend thus demands efficient energy storage (battery) equipment that possesses high durability, high energy density, and high power density, which is economically and environmentally friendly with easily available raw materials [2]. A battery that appealed to be efficient in its application in the field of renewable energy is lithium-ion batteries.

Lithium-ion batteries, however, labor under an anode problem in which the graphite contained experiences an increase in volume as the charge-discharge process takes place. The increase in volume is caused by the deposition of lithium metal on the surface of the electrode, causing an irreversible change in the volume of the crystal structure. This change in volume can damage the solid electrolyte interphase (SEI) protective layer, which can cause the continuous electrolyte decomposition, loss of Li supply, and increase cell impedance [3].

Graphite has a work potential of about 0.04 V, much lower than the electrolyte decomposition potential at 0.8 V, giving rise to the formation of a passive layer of solid electrolyte interphase (SEI) during the charging process [4]. Above the SEI layer, sharp lithium dendrite deposits will form that could potentially result in a short circuit in the lithium-ion battery.

$Li_4Ti_5O_{12}$ (LTO) material is attracting the attention of many researchers on its role in graphite anode replacement [5]. LTO has advantages, among others, of having zero strain insertion, meaning that no volume change occurs during the charge-discharge process, high flat voltage (~1.55V) that prevents electrolytes from decomposing; thus no SEI and lithium dendrites forms on the surface of the anode [3, 5], and volumetric capacity of 600 mAh/cm$^3$. Volumetric capacity is quotient of the capacity of a cell or battery by its volume. 600 mAh/cm3 is considered relatively high volumetric capacity. Conversely, LTO also possesses disadvantages of having a low rate capability due to low electronic conductivity (<$10^3$ Scm$^{-1}$), low diffusion coefficient ($10^{-9}$cm$^2$s$^{-1}$), low specific capacity (175 mAh/g) compared to graphite (375 mAh/g) [6], and experiencing production of gas ($CO_2$, $H_2$, CO) during the charge-discharge process, especially at high temperatures [7].

To overcome these deficiencies, this study explores the doping of metal ions on LTO. This effort aims to improve the electrochemical properties of LTO, especially its durability. Metal ions that can be used in LTO doping include $Mg^{2+}$, $Co^{3+}$, $Al^{3+}$, $Zr^{4+}$, $V^{5+}$, $Ta^{5+}$, $Mo^{4+}$, and others [8]. These metals are able to be used

Received June 27, 2020, Revised September 6, 2020, Accepted for publication September 22, 2020

as they have smaller ionic radii enabling them to be doped into LTO on its Li, Ti, or O atoms. The $Al^{3+}$ metal ion was especially chosen in this study as it does not change the crystal structure of the LTO [9]. $Al^{3+}$ ion doping on $Ti^{3+}$ can increase reversible capacity and cycle stability during charge-discharge process [10]. In this case, some of the $Ti^{3+}$ ions will be replaced with $Al^{3+}$ in which the standard Gibbs energy of $Al_2O_3$ ($-1576.4$ kJ $mol^{-1}$) is greater than $Ti_2O_3$ ($-1543.9$ kJ $mol^{-1}$), meaning the stability of the Al-O bond is higher than Ti-O in the octahedral coordination in LTO spinel structures [11], implying that the stability of the LTO cycle can be increased. Reversible capacity defined as the capacity after 100 cycles and represents the stable capacity that is delivered by the electrode, after the formation cycles are completed [12]. If the cycle is stable, the reversible capacity will increase. Thus, in this research, Al-doped LTO is synthesized by sol-gel method and the effects of $Al^{3+}$ doping on the capacity and diffusion coefficient of LTO on lithium ion batteries are determined.

## 2 Research Methodology

### 2.1 Materials

The synthesis of $Li_4Ti_{(5-x)}Al_xO_{12}$ (LTO-Al) anode material used technical grade lithium acetate ($C_2H_3O_2Li$), titanium (IV) butoxide ($C_{16}H_{36}O_4Ti$) p.a. Sigma Aldrich, 37% hydrochloric acid (HCl) p.a. Sigma Aldrich, aluminum acetate ($C_4H_7AlO_5$) p.a. Sigma Aldrich, and ethanol ($C_2H_5OH$) p.a. Merck as a solvent. The making of electrode sheets involve the use of LTO-Al active material, Cu-foil, technical PVDF (polyvinylidene fluoride), super P (carbon) and DMAC (N, N-dimethyl-acetamide) solvent pa Merck. The coin cell was constructed from lithium metal, $LiPF_6$ electrolyte, and a set of coin cell.

### 2.2 Instrumentation

Automatic battery cycler was used to determine the electrochemical performance of the charge-discharge capacity. Data analysis was performed with WBCS3000 software.

### 2.3 $Li_4Ti_{(5-x)}Al_xO_{12}$ synthesis

The sol-gel method was used to synthesize $Li_4Ti_{(5-x)}Al_xO_{12}$ ceramic material. To produce 2 grams of LTO/Al powder, each raw material was dissolved in ethanol along with HCl catalyst. In solution A, 6.4 ml of titanium butoxide ($C_{16}H_{36}O_4Ti$) was dissolved in 50 ml of ethanol with 2 ml of HCl catalyst. Moreover, in solution B, 1.2041 grams of lithium acetate ($C_2H_3O_2Li$) was dissolved in 15 ml of ethanol with 0.5 ml of catalyst HCl, whereas solution C used aluminum acetate ($C_4H_7AlO_5$) with concentration variations of 1.5%; 3%; 4.5%, dissolved in 15 ml of ethanol and 0.5 ml of HCl catalyst. The mass of aluminum acetate for Al doping variations (0%, 0.5%, 1.5%, 3%, and 4.5%) which formulated from stoichiometric calculation are 0 g, 0.0039 g, 0.0106 g, 0.0218 g, 0.0313 g respectively. The first combination of solution entailed the dripping of solution B into solution A. Subsequently, solution C was added dropwise into the mixture of solution A and B followed by stirring for 12 hours to form a clear solution. The sample was dried in an oven at 80°C for 24 hours. The obtained LTO/Al precursor was sintered in a furnace at 850°C for 4 hours under air atmosphere to obtained Al-doped LTO white powder.

### 2.4 Measurement of electrochemical properties

The LTO/Al anode slurry used active material composition ratio of (LTO/Al) 80%: PVDF (polyvinylidene fluoride) 10%: Super P (carbon) 10% making up 0.50 gr active material. Additionally, 2 mL of DMAC (dimethyl acetamide) was used as a solvent. Material mixing was carried out at 70°C with stirring at 250 rpm. Furthermore, the slurry is made into sheets by being poured onto the surface of Cu foil using a doctor blade with a thickness of 150 μm and dried at 80°C for 1 hour. The dried anode sheet was then cut into a circle with a diameter of 16 mm. The cells were assembled using electrode sheets as working electrode, lithium metal as the counter electrode, Celgard film as the separator, and $LiPF_6$ dissolved in organic solvent, i.e., ethylene carbonate (EC) and diethyl carbonate (DEC) was used as electrolyte. The coin cell was assembled in a glove box filled with Ar (argon) gas. The coin cell arrangement can be seen in Figure 1.

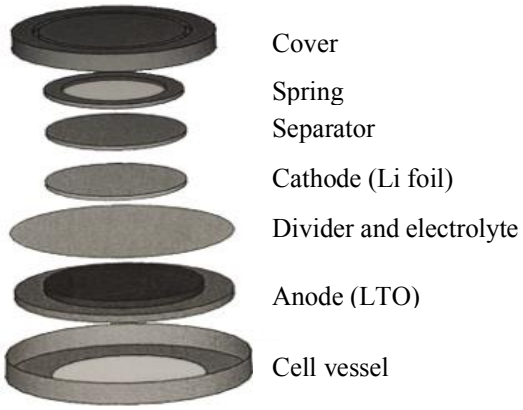


**Figure 1** Coin cell composition

Electrochemical performance was tested using automatic battery cycler and WBCS 3000 software. Cyclic voltammetry was performed by varying the scan rate (100,200,300,400,500 μV/s) with a voltage range of 1-2.5 V.

## 3 Results and Discussion

In this study, Al-doped LTO was synthesized using the sol gel method. The sintering process produced white LTO/Al powder which was then made into LTO/Al sheets shown in Figure 2. The effect of Al doping on the diffusion coefficient and capacity of LTO in lithium ion batteries was analyzed using cyclic voltammetry and WBCS 3000.

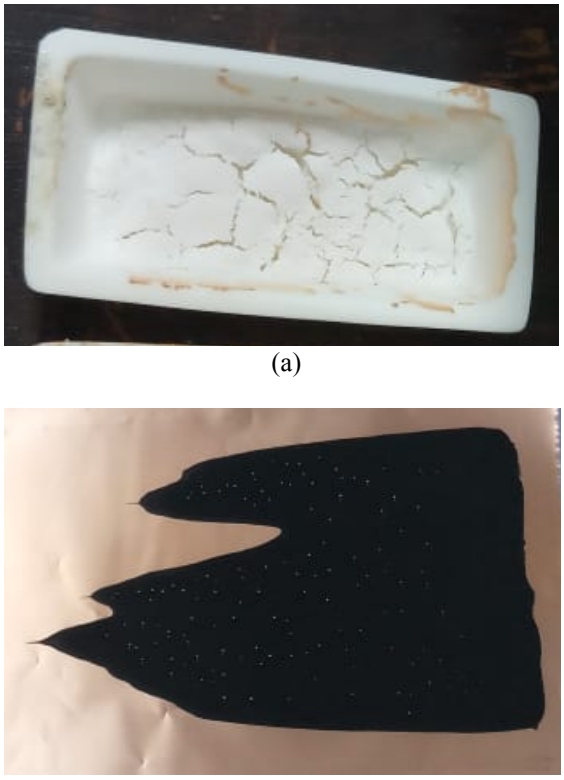

(a)

(b)

**Figure 2** a) LTO/Al powder and b) LTO/Al sheet

Figure 3 shows the cyclic voltammetry curve in LTO doped with Al at varying concentrations (0%; 0.5%; 1.5%; 3%; 4.5%), tested with a variation of scan rate of 100-500 µV/s at voltages within 1-2.5 V. In testing with different scan rates, all samples show an oxidation peak at 1.7 V and a reduction peak at 1.5 V indicating charge-discharge and reversible processes. The cathode peak (reduction) denotes the discharge process, while the anode peak (oxidation) denotes the charge process of the sample followed by a redox reaction $Ti^{4+}$ /$Ti^{3+}$ related to the following reaction [9]:

$$Li_4Ti_5O_{12} + 3Li^+ + 3e^- \leftrightarrow Li_7Ti_5O_{12} \quad (1)$$

Oxidation peaks and reduction peaks appear higher along with the increase in scan rate in the four samples, showing that more flux of the $Li^+$ ion electrodes moves from the anode to the cathode. All four graphs have shifts in curves at different rates. At low scan rates, electrolyte ions and the active material (LTO/Al) have sufficient time to interact with each other increasing the likelihood of a redox reaction, but at high scan rates, this interaction does not take place perfectly due to lack of time to interact.

Cyclic voltammetry curves are influenced by kinetic and diffusion processes [13]. If the redox process is affected by diffusion, the potential peak will not be affected by the scan rate. Meanwhile, if the redox process is influenced by a kinetic process, the scan rate will affect the entire voltammetry curve, especially at the potential peak [13]. The doping of $Al^{3+}$ metal ions decreases current value as $Al^{3+}$ doping inhibits the diffusion of $Li^+$ ions and especially in the diffusion of electrons produced in anode, thereby reducing the intensity of current curve peak.

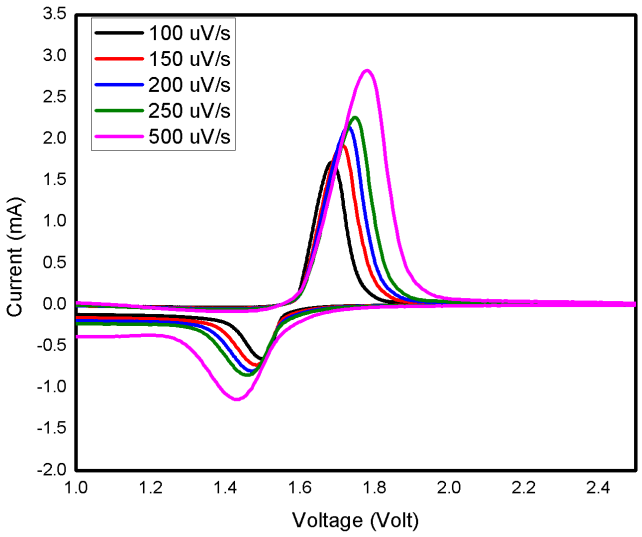


(a)

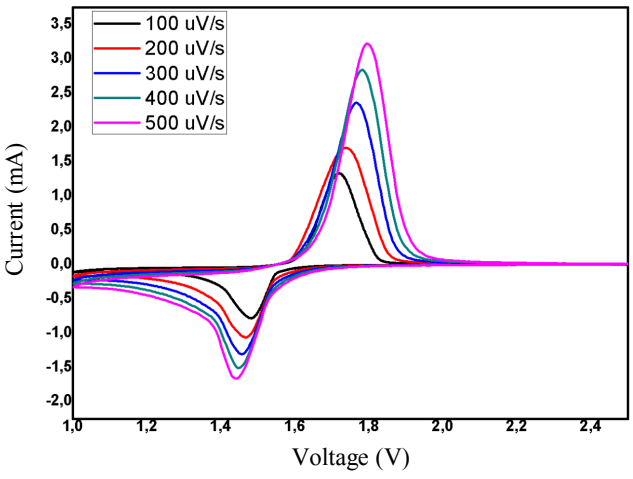


(b)

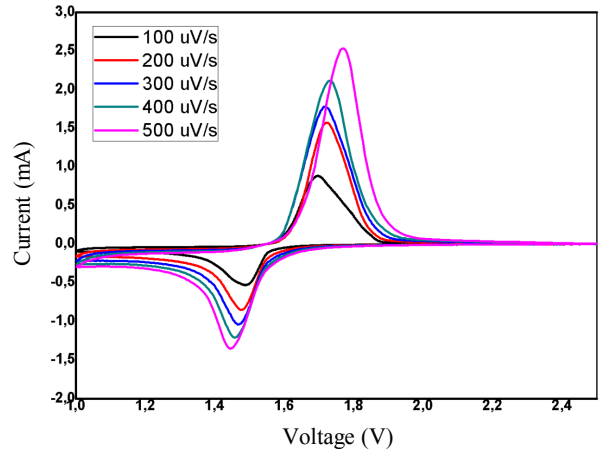


(c)

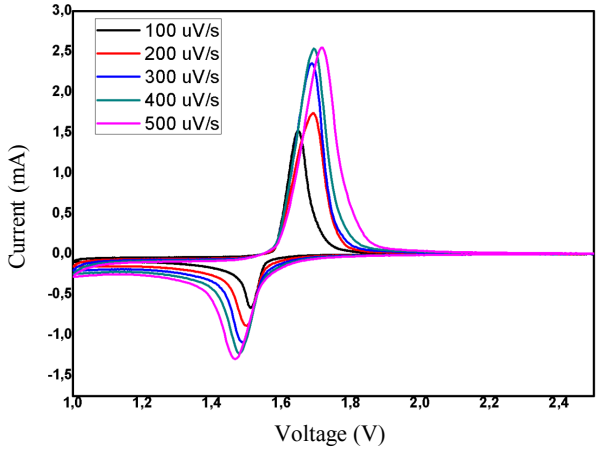


(d)

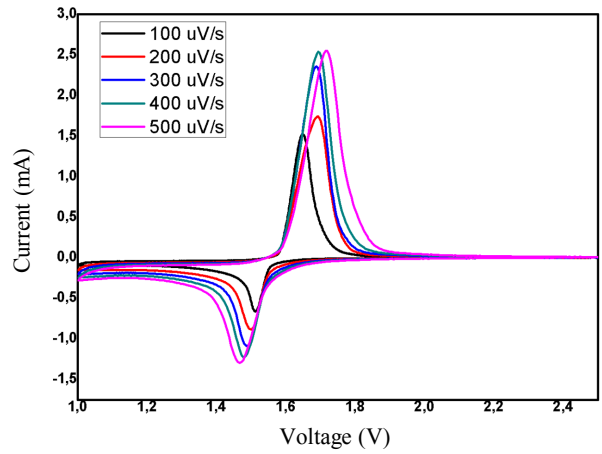


(e)

**Figure 3** Cyclic voltammetry curve of LTO/Al with Al doping variations of a) 0%, b) 0.5%, c) 1.5%, d) 3%, and e) 4.5% at different scan rates 100-500 µV/s

Lithium ions migrate from the cathode via electrolyte to the anode. The separator is between the two electrodes and functions as a lithium ion transfer medium during the charging and discharging processes. The pore size of the separator provides sufficient space for electrolyte adsorption ensuring fast percolation of lithium ions through the separator while preventing short circuit and self-discharge [14] The $Li^+$ ion diffused from the cathode (lithium metal) to the anode (LTO/Al) at 1.5 V consequentially bringing the curve to a rise. When it reached the peak, the amount of Li ions diffusing into the anode caused the accumulation of $Li^+$ ions causing the curve to decrease because $Li^+$ could not encounter electrons from the Cu-foil. When the peak current decreases, the diffusion coefficient value also decreases.

From the voltage and peak current data of the redox reaction, the magnitude of the diffusion coefficient of Li ions can be calculated by using the Randles-Sevcik equation [15] as follows:

$$I_{pa/pk} = 0{,}4463AC(n^3F^3vD/RT)^{1/2} \text{ (at } 25^oC) \qquad (2)$$

where $I_{pa/pk}$ is the peak current of the cathode or anode; n is the number of electrons; A is the anode surface area; C is the lithium ion concentration; D is the diffusion coefficient of lithium ion, and v is the scan rate. To calculate the diffusion coefficient, it is necessary to graph the oxidation current (Ip) vs $\sqrt{v}$ as shown in Figure 4.

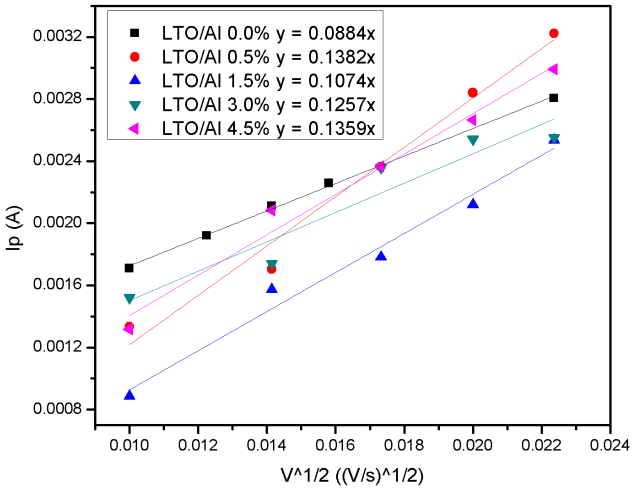


**Figure 4** Linear graphs of LTO/Al sample

Table 1 presents the diffusion coefficient (D) of the LTO/Al samples (0%; 0.5%; 1.5%; 3%; 4.5%) respectively at 0.52047x$10^{-10}$ $cm^2/s$; 1.24646 x$10^{-10}$ $cm^2/s$; 0.7674 x$10^{-10}$ $cm^2/s$; 1.0551 x$10^{-10}$ $cm^2/s$; 1.224 x$10^{-10}$ $cm^2/s$. The best diffusion coefficient belongs to the 0.5% LTO/Al sample. Small amount of ions are needed in the doping process to be able to improve the electrochemical performance of lithium batteries, however, in a circumstance where more ions are used, a decrease in the peak current value and diffusion coefficient can occur [16].

Battery capacity is the amount of energy that can contained and released by a battery [17]. Energy or charge capacity is expressed in units of mAh/gram. Figure 5 shows the Charge-Discharge curve in LTO doped with Al (0%; 0.5%; 1.5%; 3%; 4.5%), tested at a scan rate range of 100-500 µV/s at 1 – 2.5 V. All four samples have a charge voltage of 1.6 V and a discharge voltage of 1.5 V. The charge capacity appears to increase when the voltage is 1.6 V, while the discharge capacity decreases when the voltage is 1.5 V in all samples. As seen on the four curves displayed, higher scan rate (100-500 µV/s) decreases capacity. This is due to lesser time available for the interactions of lithium ions with electrons, meaning that the number of electrons stored in the battery is smaller. Increasing the scan rate also increases the polarization voltage. It can be look from voltage difference between cathodic and anodic when increasing charge-discharge rate. The polarization voltage is the difference between the charging and the discharging voltages. The polarization voltage arises due to the activation process, the difference in concentration on the surface of the electrode as a result of mass transfer, and the resistance of the electrode material.

**Table 1** Diffusion coefficient of LTO/Al

| Sample | Scan rate (µV/s) | $V_{oxidation}$ (V) | $I_p$ (mA) | $D_{Li}$ ($cm^2/s$) |
|---|---|---|---|---|
| **0%** | 100 | 1.6853 | 1.7087 | $0.52047 \times 10^{-10}$ |
| | 150 | 1.7093 | 1.9197 | |
| | 200 | 1.7353 | 2.1112 | |
| | 250 | 1.7498 | 2.2569 | |
| | 500 | 1.7831 | 2.8052 | |
| **0.5%** | 100 | 1.7189 | 1.3336 | $1.26464 \times 10^{-10}$ |
| | 150 | 1.7378 | 1.7049 | |
| | 200 | 1.7666 | 2.3629 | |
| | 250 | 1.7834 | 2.8407 | |
| | 500 | 1.7941 | 3.223 | |
| **1.5%** | 100 | 1.6953 | 0.88515 | $0.7674 \times 10^{-10}$ |
| | 150 | 1.7211 | 1.5743 | |
| | 200 | 1.7174 | 1.781 | |
| | 250 | 1.7293 | 2.1193 | |
| | 500 | 1.7669 | 2.5359 | |
| **3.0%** | 100 | 1.6504 | 1.5204 | $1.051 \times 10^{-10}$ |
| | 150 | 1.6931 | 1.7404 | |
| | 200 | 1.6887 | 2.3579 | |
| | 250 | 1.6932 | 2.5402 | |
| | 500 | 1.7196 | 2.5512 | |
| **4.5%** | 100 | 1.6893 | 1.3179 | $1.224 \times 10^{-10}$ |
| | 150 | 1.712 | 2.084 | |
| | 200 | 1.7042 | 2.366 | |
| | 250 | 1.7201 | 2.6649 | |
| | 500 | 1.7547 | 2.9927 | |

The capacity in each sample (0; 0.5; 1.5; 3; 4.5)% varies, among others 88.9303 mAh/g; 81.5898 mAh/g; 74.9334 mAh/g; 84.4289 mAh/g; 75.4795 mAh/g. The capacity values do not differ greatly from experiments conducted by Krajewski et al [18] at around 80 mAh/g. The small capacity value is caused by the Al doped into the material inhibiting the diffusion of Li ions. The highest charge-discharge capacity values are found in the 0% LTO/Al anode with respective charge and discharge values of 88.9303 mAh/g and 77.864 mAh/g.

A battery can be said to be efficient when its ability to store energy (charge capacity) is equivalent to its ability to release them (discharge capacity) [19]. Table 2 shows that the values of the charge and discharge capacity as well as the coulombic efficiency in the four LTO/Al samples are only around 80% since the charge-discharge process was only run up to 1 V.

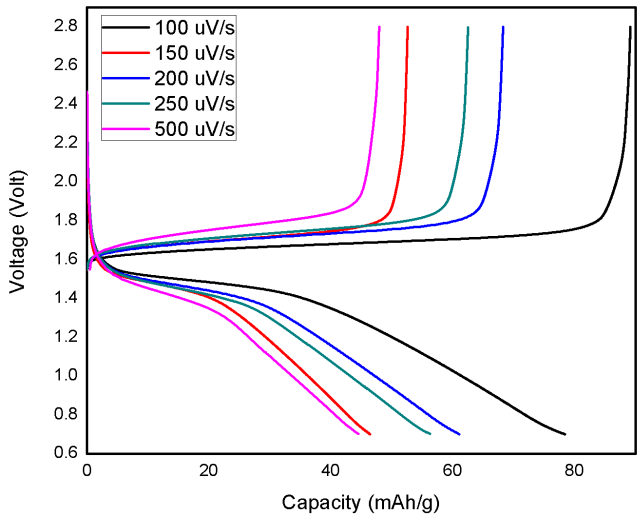


(a)

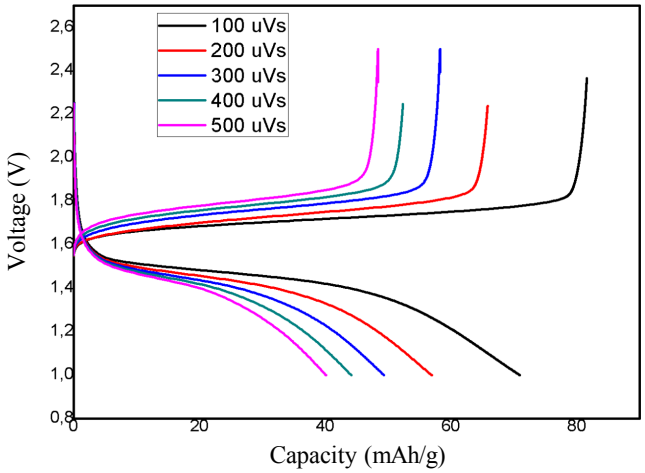


(b)

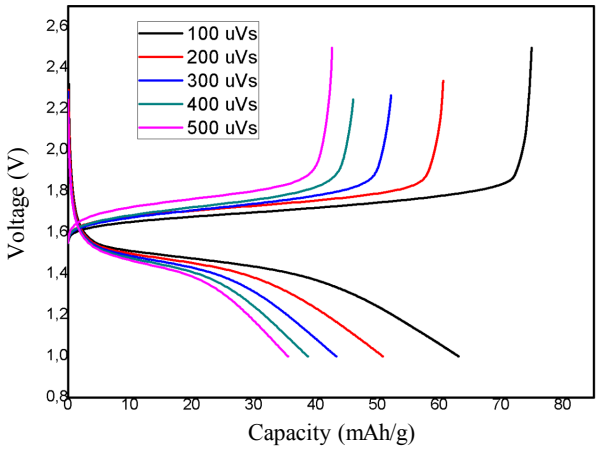


(c)

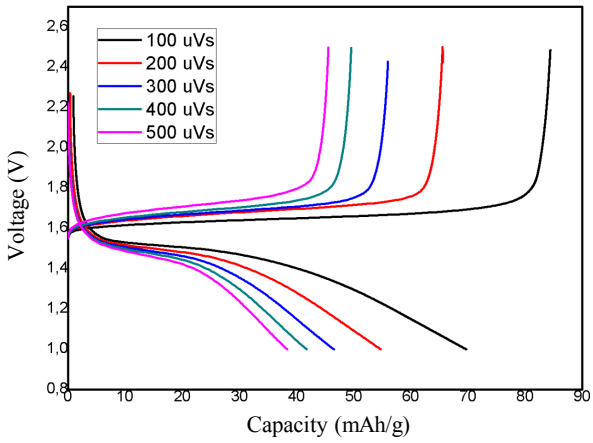


(d)

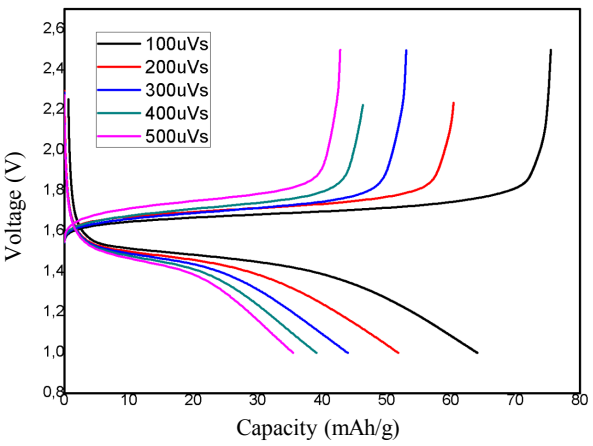


(e)

**Figure 5** Charge-discharge curve of LTO/Al with Al concentrations of b) 0.5%, c) 1.5%, d) 3%, and e) 4.5% at different scan rates (100-500 µV/s)

**Table 2** Charge-discharge capacity of LTO/Al

| Sample | Scan rate (µV/s) | Capacity | | Coulombic Efficiency (%) |
|---|---|---|---|---|
| | | Charge | Discharge | |
| **0%** | 100 | 88.9303 | 77.864 | 87.55 |
| | 150 | 68.2572 | 60.9496 | 89.29 |
| | 200 | 62.4091 | 56.1412 | 89.95 |
| | 250 | 52.5924 | 46.1246 | 86.06 |
| | 500 | 48.0039 | 44.2452 | 92.17 |
| **0.5%** | 100 | 81.5898 | 70.526 | 86.43 |
| | 150 | 65.8099 | 56.9352 | 86.51 |
| | 200 | 58.2887 | 49.3634 | 84.69 |
| | 250 | 52.3504 | 44.1345 | 84.31 |
| | 500 | 48.4155 | 40.1378 | 82.90 |
| **1.5%** | 100 | 74.9334 | 63.1678 | 84.29 |
| | 150 | 60.6309 | 50.8992 | 83.95 |
| | 200 | 52.209 | 43.3402 | 83.01 |
| | 250 | 46.1113 | 38.77 | 84.08 |
| | 500 | 42.6797 | 35.5521 | 83.30 |
| **3.0%** | 100 | 84.4289 | 69.6814 | 82.53 |
| | 150 | 65.6054 | 54.7377 | 83.43 |
| | 200 | 55.9975 | 46.5108 | 83.06 |
| | 250 | 49.5711 | 41.7691 | 84.26 |
| | 500 | 45.5735 | 38.3495 | 84.15 |
| **4.5%** | 100 | 75.4795 | 64.069 | 84.88 |
| | 150 | 60.3825 | 51.8019 | 85.79 |
| | 200 | 53.0354 | 43.9531 | 82.87 |
| | 250 | 46.2985 | 39.109 | 84.47 |
| | 500 | 42.7873 | 35.5058 | 82.98 |

## 4 Conclusion

A variation of $Li_4Ti_5O_{12}$ variation doped with Al (0.5%; 1.5%; 3%; 4.5%) was successfully synthesized through the sol-gel method. Doping of $Al^{3+}$ metal ions is able to influence the electrochemical performance (diffusion coefficient and capacity) of a battery. The diffusion coefficient (D) of the LTO/Al samples (0%; 0.5%; 1.5%; 3%; 4.5%) respectively at 0.52047x$10^{-10}$ $cm^2/s$; 1.24646 x$10^{-10}$ $cm^2/s$; 0.7674 x$10^{-10}$ $cm^2/s$; 1.0551 x$10^{-10}$ $cm^2/s$; 1.224 x$10^{-10}$ $cm^2/s$. The capacity in each sample (0%; 0.5%; 1.5%; 3%; 4.5%) varies, among others 88.9303 mAh/g; 81.5898 mAh/g; 74.9334 mAh/g; 84.4289 mAh/g; 75.4795 mAh/g. The higher Al doping in LTO, the lower the diffusion coefficient and capacity.

## Acknowledgment

This article is partially supported by USAID through Sustainable Higher Education Research Alliances (SHERA) Program.

## References


[1] M. A. Hannan, M. S. H. Lipu, A. Hussain, and A. Mohamed, "A review of lithium-ion battery state of charge estimation and management system in electric vehicle applications: Challenges and recommendations," *Renew. Sustain. Energy Rev.*, vol. 78, no. August 2016, pp. 834–854, 2017.

[2] L. Lu, X. Han, J. Li, J. Hua, and M. Ouyang, "A review on the key issues for lithium-ion battery management in electric vehicles," *J. Power Sources*, vol. 226, pp. 272–288, 2013.

[3] N. Nitta, F. Wu, J. T. Lee, and G. Yushin, "Li-ion battery materials: Present and future," *Mater. Today*, vol. 18, no. 5, pp. 252–264, 2015.

[4] F. Wu *et al.*, "Low-temperature synthesis of nano-micron Li 4Ti 5O 12 by an aqueous mixing technique and its excellent electrochemical performance," *J. Power Sources*, vol. 202, pp. 374–379, 2012.

[5] A. Sohib *et al.*, "Electrochemical performance of low concentration Al doped-lithium titanate anode synthesized via sol-gel for lithium ion capacitor applications," *J. Energy Storage*, vol. 29, no. April, p. 101480, 2020.

[6] S. Zhang, X. Ge, and C. Chen, "Synthesis of carbon-coated Li4Ti5O12 and its electrochemical performance as anode material for lithium-ion battery," *Chinese Chem. Lett.*, vol. 28, no. 12, pp. 2274–2276, 2017.

[7] A. I. Najihah, "Optimalisasi waktu tahan kalsinasi pada sintesis material anoda Li4Ti5O12 dengan metode sol-gel," *Skripsi, Fak. Mat. dan Ilmu Pengetah. Alam, UNNES*, vol. 11, no. 4, pp. 365–370, 2014.

[8] T. F. Yi, L. J. Jiang, J. Shu, C. B. Yue, R. S. Zhu, and H. Bin Qiao, "Recent development and application of Li4Ti5O 12 as anode material of lithium ion battery," *J. Phys. Chem. Solids*, vol. 71, no. 9, pp. 1236–1242, 2010.

[9] S. Priyono, J. Triwibowo, and B. Prihandoko, "The effect of 0.025 Al-doped in Li4Ti5O12 material on the performance of half cell lithium ion battery," *AIP Conf. Proc.*, vol. 1711, pp. 1–7, 2016.

[10] H. Zhao, Y. Li, Z. Zhu, J. Lin, Z. Tian, and R. Wang, "Structural and electrochemical characteristics of Li4-xAlxTi5O12 as anode material for lithium-ion batteries," *Electrochim. Acta*, vol. 53, no. 24, pp. 7079–7083, 2008.

[11] S. Huang, Z. Wen, Z. Gu, and X. Zhu, "Preparation and cycling performance of Al3+and F- co-substituted compounds Li4AlxTi5-xF yO12-y," *Electrochim. Acta*, vol. 50, no. 20, pp. 4057–4062, 2005.

[12] W. Li, R. Yang, J. Zheng, and X. Li, "Tandem plasma reactions for Sn/C composites with tunable structure and high reversible lithium storage capacity," *Nano Energy*, vol. 2, no. 6, pp. 1314–1321, 2013.

[13] M. Matsumiya, M. Terazono, and K. Tokuraku, "Temperature dependence of kinetics and diffusion coefficients for ferrocene/ferricenium in ammonium-imide ionic liquids," *Electrochim. Acta*, vol. 51, no. 7, pp. 1178–1183, 2006.

[14] A. Reizabal, R. Gonçalves, C. M. Costa, L. Pérez, and L. Vilas, "Tailoring silk fibroin separator membranes pore size for improving performance of lithium ion batteries," *J. Memb. Sci.*, p. 117678, 2019.

[15] C. Han *et al.*, "Suppression of interfacial reactions between Li4Ti5O12 electrode and electrolyte solution via zinc oxide coating," *Electrochim. Acta*, vol. 157, pp. 266–273, 2015.

[16] T. V. S. L. Satyavani, A. Srinivas Kumar, and P. S. V. Subba Rao, "Methods of synthesis and performance improvement of lithium iron phosphate for high rate Li-ion batteries: A review," *Eng. Sci. Technol. an Int. J.*, vol. 19, no. 1, pp. 178–188, 2016.

[17] D. P. Kosasih, "Pengaruh Variasi Larutan Elektrolite Pada Accumulator Terhadap Arus Dan Tegangan," *MESA J. Fak. Tek. Univ. SUBANG*, no. Vol. 2 No. 2 (2018): MESA (Teknik Mesin, Teknik Elektro, Teknik Sipil, Teknik Arsitektur), pp. 33–45, 2018.

[18] M. Krajewski, B. Hamankiewicz, M. Michalska, M. Andrzejczuk, L. Lipinska, and A. Czerwinski, "Electrochemical properties of lithium-titanium oxide, modified with Ag-Cu particles, as a negative electrode for lithium-ion batteries," *RSC Adv.*, vol. 7, no. 82, pp. 52151–52164, 2017.

[19] E. M. Wigayati, I. Purawiardi, and Q. Sabrina, "Karakteristik Morfologi Permukaan Pada Polimer PVdF-LiBOB-ZrO2 dan Potensinya untuk Elektrolit Baterai Litium," *J. Kim. dan Kemasan*, vol. 40, no. 1, p. 1, 2018.